

# Characterisation of actuation properties of piezoelectric bi-stable carbon-fibre laminates

P. Giddings, C.R. Bowen \*, R. Butler, H.A. Kim

*Department of Mechanical Engineering, University of Bath, Bath, Somerset BA2 7AY, UK*

Received 30 March 2007; received in revised form 25 June 2007; accepted 27 July 2007

## Abstract

This paper characterises the properties of bi-stable carbon fibre composites actuated using a macro fibre piezoelectric actuator. An unsupported piezoelectric–laminated combination was evaluated in terms of its blocking force, free displacement and load–displacement characteristics. Linear relationships between blocking force and free displacement with applied voltage were observed when the piezoelectric–laminated combination was actuated in a single stable state. The load–deflection characteristics indicate that significant control of the snap-through force could be achieved with applied voltage.

© 2007 Elsevier Ltd. All rights reserved.

*Keywords:* A. Laminates; A. Smart materials; B. Mechanical properties; B. Electrical properties

## 1. Introduction

There is increasing interest in structures that can change shape (or morph), particularly for structural adaptation concepts in aerospace applications [1,2]. Of the different methods considered, those using bi-stable composites [3–11] demonstrate some of the most interesting properties; notably the ability to generate large changes in shape without the need for a continuous power supply [3].

A bi-stable composite laminate exhibits two distinct structurally-stable deformation states. The most common class of bi-stable laminates is the unsymmetric cross-ply laminate, the bi-stability of which was first reported by Hyer [12]; these laminates exhibit cylindrical curvature of opposite sign about generators that lie parallel to the fibre directions and hence perpendicular to one another.

There is a significant difference in coefficient of thermal expansions (CTE) of the reinforcing fibres and polymer matrix materials resulting in anisotropic laminate CTE

[10,13]. Upon cooling from the elevated cure temperature, the resulting difference in thermal contraction creates a residual stress state that is the cause of the observed laminate curvatures [10,14,15].

Classical lamination theory (CLT), based on the Kirchhoff hypothesis, predicts that unsymmetric laminates develop into a saddle-shape during post-cure cooling. However, as hypothesised [12] and later confirmed by Hyer [16] laminates with high edge-length to thickness ratios do not generally form stable saddle shaped laminates. In these laminates, geometric non-linearities along with large out-of-plane deformations prevent the saddle-shape being structurally stable, instead one of two cylindrical states is observed [12,17]. These effects are not accounted for in CLT and hence the occurrence of cylindrical deformation is not predicted.

It has been demonstrated that it is possible to switch between stable states (induce ‘snap-through’) by superposing an adaptive stress state onto the residual stress state of the bi-stable composite [7]. Actuator materials such as shape memory alloys [6,7,12] or piezoelectric [3–6] materials have been used to develop the adaptive stress to induce

\* Corresponding author. Tel.: +44 1225 383660.  
E-mail address: [C.R.Bowen@bath.ac.uk](mailto:C.R.Bowen@bath.ac.uk) (C.R. Bowen).

‘snap-through’ and generate large overall deflections and changes in shape of the structure. The actuator materials are generally bonded onto the outer surface of the composite [3–6] and less work has considered, or attempted, to fully integrate the actuator material into the composite structure [7,18].

It is unusual for an actuator or adaptive structure to actuate or change shape in the absence of an externally applied mechanical load. In addition, it has been recently demonstrated that combined piezoelectric and mechanical loading could offer a practical solution to achieve reversible snap-through and control the morphing of bi-stable composite structures [9]. Appreciable reversible deflections and shape change can also be achieved by simply maintaining the unsymmetrical composite structures in a single stable configuration [9].

Theoretical analysis of bi-stable laminates and the prediction of shapes has been examined by several investigators. Hyer [16] first formulated an extension to CLT including geometric non-linearities normally used in thin-plate theory to predict room temperature shapes of bi-stable laminates. Hyer’s technique also assumed simple polynomial out of plane displacement fields within the Rayleigh Ritz minimisation. Dang and Tang [19], Jun and Hong [20] among other investigators [21–24] extended Hyer’s 1981 work [16] with more complex polynomial displacement fields to predict room temperature shapes of more general laminates. This area is now well developed and laminate behaviour can be accurately predicted. The problem of modelling piezo-electrically actuated morphing and snap-through however is less understood.

Schultz and Hyer [3] developed a multi-stage method for modelling the behaviour and snap-through voltage of an MFC actuated cross-ply laminate. Ren [25] later developed a single stage modelling technique for MFC actuated cross-ply laminates that was verified by FEA modelling.

Experimental verification of these models and of the behaviour of piezoelectrically actuated bi-stable laminates in general is less well developed. Schultz and Hyer [3] and Hufenbach [6] have measured the voltage required to induce snap-through in a laminate resting on a plane surface, while Dano and Hyer [26] have undertaken analogous work for thermally actuated laminates. Asanuma [27] has investigated actuation properties of a thermally-actuated active laminate, however, it is not known how piezoelectrically actuated bi-stable laminates behave during actuation within a single stable state, or during snap-through events.

This paper aims to characterise a piezoelectrically actuated bi-stable carbon-fibre laminate in terms of free deflection, blocking force and load–deflection behaviour within a single deformation state. Force–displacement behaviour of the laminate under combined electrical and mechanical loading during deformation and snap-through are also characterised. Theoretical explanations based on current modelling techniques are also presented for the observed results.

## 2. Experimental

### 2.1. Composite manufacture and actuator attachment

An unsymmetric  $[0/90]_T$  carbon fibre/epoxy composite measuring  $150 \times 150 \times 0.32 \text{ mm}^3$ , similar to that examined by Schultz and Hyer [3], was manufactured to operate as an unsupported laminate. The composite lay-up procedure was a standard method for manufacturing carbon laminates using carbon fibre pre-preg sheet (HTA (12k) 913). The samples were laid on a non-stick pad to ensure that the composite would not bond to the lay-up surface during the cure cycle. Once the layers had been placed a thermocouple was inserted into the pre-preg plies to monitor the laminate temperature during the cure cycle. Release film was placed over the sample and a breather layer was laid to assist in forming the vacuum during curing. The laminate was run through a standard cure cycle to a maximum cure temperature of  $125 \text{ }^\circ\text{C}$  and a pressure  $\sim 0.6 \text{ MPa}$ .

The piezoelectric material used was a macro fibre composite (MFCs) from Smart Material Corporation, USA, which consists of aligned piezoelectric fibres with an interdigitated electrode to direct the applied electric field along the fibre axis. A relatively large MFC patch (M-8557-P1) was used ( $110 \times 75 \text{ mm}^2$ ) with an active area of  $85 \times 57 \text{ mm}^2$  and an electrode spacing of  $0.5 \text{ mm}$ . The material used for the MFC was a Navy Type II lead zirconate titanate (PZT). The maximum operating voltage was  $1500 \text{ V}$  (biased to the poling direction) with a maximum reported free strain per volt of  $0.75 \text{ ppm/V}$  at electric low field ( $<1 \text{ kV/mm}$ ) and  $0.9 \text{ ppm/V}$  at high field ( $>1 \text{ kV/mm}$ ) [18]. Table 1 provides typical properties of the carbon fibre material and macro fibre composite.

A two-part araldite epoxy was used to bond the MFC actuator to the laminate. The surfaces of the actuator and carbon fibre composite were cleaned and the surface of the composite roughened to provide better mechanical adhesion. A small quantity of the adhesive was applied to the actuator and was evenly spread on its surface to form as thin a film as possible and ensure good strain transfer between the actuator and composite. Once attached to the composite, the actuator and composite were placed beneath a weight to keep the composite and actuator flat and in good contact for  $24 \text{ h}$  while the epoxy cured. Due to the applied load during bonding, the actuator was

Table 1  
Material properties of composite and MFC (from Smart Material Corporation)

	HTA (12k) 913	Piezoelectric MFCs
$E_{11}$ (GPa)	135	30.3
$E_{22}$ (GPa)	18.5	15.9
$G_{12}$ (GPa)	5.98	5.51
$\nu_{12}$	0.29	0.31
Free strain per volt ( $10^{-6}/\text{V}$ )	–	0.75–0.90 (low field–high field)
% Strain @ $1500 \text{ V}$	–	0.11–0.135

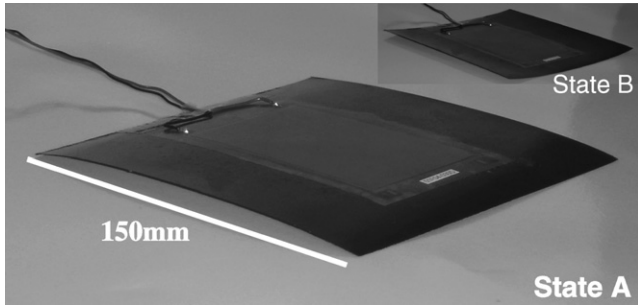


Fig. 1. Composite in state A with MFC attached. The inset shows the second stable state (state B).

bonded to the laminate whilst held flat, with the direction of the main actuator strain (and its piezoelectric fibres) aligned along the axis of curvature. The actuator–composite lay-up is therefore  $[0_{\text{MFC}}/0/90]_{\text{T}}$ . Fig. 1 shows the composite with the actuator attached. Attaching the actuator to the laminate whilst held flat resulted in a final piezoelectric–laminate combination with a smaller degree of curvature compared to the initial laminate. However the composite remained bi-stable and exhibited two stable states (state A and state B), as shown in Fig. 1.

## 2.2. Blocking force

The blocking force is regarded as the maximum force exerted by an actuator when placed in a perfectly unyielding clamp [28]. To determine the relationship between applied voltage and blocking force the test rig shown in Fig. 2 was designed to allow force measurement in an Instron 1122 mechanical test machine. The rig consisted of two smooth support rails screwed into an aluminium top-plate which was supported by four round aluminium columns. These columns were bolted into both top and base-plates, with the base plate bolted to an Instron mount-

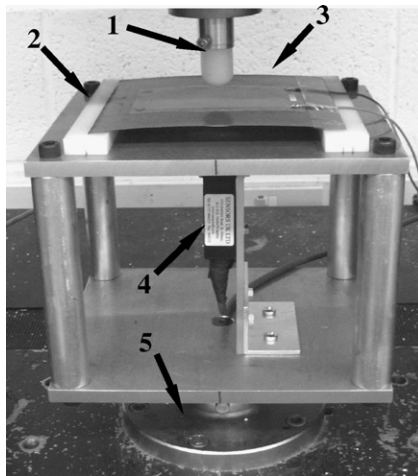


Fig. 2. Test rig to determined blocking force, free deflection and force–deflection characteristics. (1) Nylon cross-head; (2) nylon support rails; (3) composite in state A; (4) laser displacement sensor; (5) standard Instron boss.

ing boss. The laminate support rails and the cross-head of the Instron load cell were machined from nylon to provide electrical isolation of testing equipment from the applied voltage (up to 1400 V).

A function generator was used to provide sinusoidal AC input-signals of varying amplitudes to a power amplifier (TREK PZD700 piezo driver). All signals were positively DC-biased by half the amplitude, hence all signals cycled from zero volts to a maximum voltage of 1400 V to maintain polarity of the MFC. The laminate was placed on the support rails in state A (as in Fig. 2) with no applied voltage and the cross-head of the Instron was adjusted to just contact the top of the laminate and was fixed in position. A test frequency of 0.01 Hz was selected for characterisation of blocking force, since this produced a corresponding force which alternated from 0 N (at 0 V) to a maximum force at the maximum applied voltage with limited phase difference between applied force and measured load. The applied AC voltage and resulting force were logged for 150 s. The input was then disconnected and the sample allowed to relax to its pre-test state. This procedure was repeated with the input AC voltage adjusted to measure the upward blocking force from 200 to 1400 V in 200 V increments.

## 2.3. Free deflection

Free deflection is defined as the actuator deflection in the absence of any restraining force. To undertake this experiment the test rig included a Nippon LAS 5010 V laser measurement system (see Fig. 2) to measure the centre point deflection of the laminate with voltage (with the nylon cross-head moved away from the laminate). The measurement resolution of the LAS 5010 V was 10  $\mu\text{m}$  over a 50 mm range. The laser was calibrated using a scribe table to define a datum plane; this datum was co-planar with the support surfaces of the nylon rails. Laminate centre deflection ( $w$ ) and applied voltage ( $V$ ) were measured whilst the composite was in state A and logged at 1 Hz. The displacement ( $d$ ) is defined as the central displacement at voltage  $V$  relative to its original position at 0 V. The applied voltage was increased from 0 to 1400 V in increments of 200 V. At each 200 V increment the voltage was held constant for 60 s to determine any time dependency of the laminate displacement. The application of the voltage, which increases the length of the MFC actuator in the fibre direction, led to an increase in the curvature of the piezoelectric–laminate combination and an increase in the centre deflection of the composite [9].

## 2.4. Force–deflection behaviour

The test fixture was also used to test the laminate under simultaneous mechanical and electrical loads to examine the influence of voltage on stiffness and snap-through behaviour of piezoelectric–laminate combination. The load was applied by the nylon cross-head in the centre of the

laminates and the laser used to quantify laminate deflection (thus removing inaccuracies caused by machine deflection). The laminate was placed on the support rails in state A and the nylon cross-head adjusted to within 1 mm of the laminate surface. The cross-head was then lowered at 1 mm/min and data was recorded at a sample rate of 10 Hz. All tests were performed in an initial state A position until snap-through of the piezoelectric–laminate combination to state B. Tests were performed at applied voltages between 0 and 1400 V in 200 V increments. These data were used to plot force–deflection curves for all applied voltages to examine the influence of voltage on effective stiffness and snap-through force.

### 3. Results and discussion

The three types of testing method will now be described. Firstly, the cross-head is fixed and in contact with the laminate to evaluate the ‘blocking force’ with voltage. Secondly, the cross-head is moved away from the laminate to measure the ‘free deflection’ with voltage. This blocking force and free deflection data are then combined to generate a ‘force-generation versus displacement’ diagram. The third test is to lower the cross-head at a constant rate to induce snap-through of the laminate from state A to state B.

#### 3.1. Blocking force

Fig. 3 shows the relationship between applied voltage and blocking force to be approximately linear with a correlation factor ( $R^2$ ) of 0.99. The linear relationship can be understood by a mechanical assessment of the system (see inset of Fig. 3). Assuming that the supporting edges of the laminate behave as though they are pin-jointed, the laminate may be considered as simply supported.

Due to the fixed cross-head position and static nature of blocking force testing, the laminate may be simplified as a 1D beam subject to a mid-span point loading. From the beam equation [29] for a beam of span  $L$ , stiffness  $E$  and a second moment of area  $I$ , it can be seen from Eq. (1) that there is a linear relationship between the strain ( $\epsilon$ ) at the upper surface of the beam (where the MFC is attached) and applied load ( $F$ ).

$$\epsilon = \frac{FLy}{4EI} \quad (1)$$

where  $y$  is the distance from the neutral axis. Considering Eq. (1) it can be seen that the influence of the MFC is to induce a strain at the upper surface of the laminate which in turn develops the force ( $F$ ) which will be directly proportional to the piezoelectric strain and voltage.

Leakage current from the MFC into the laminate was measured during application of 1400 V and found to be less than 0.01 mA. Temperature change of the MFC during excitation at 1400 V was measured by calibrated Infrared thermography and found to be 0.2 K over 60 s, the carbon laminate experienced a temperature change of approximately 0.15 K in this time.

#### 3.2. Free deflection

The centre displacement ( $d$ ) of the piezoelectric–laminate combination in state A, 1 and 60 s after the application of each 200 V increment is shown in Fig. 4a. Under the test conditions centre displacement is equal to the laminate free deflection as defined in Section 2.3. The application of a voltage to the MFC leads to an increase in the curvature of the laminate and hence the free deflection increases linearly with applied voltage. As shown by Ren [25], laminate curvature ( $k$ ) is proportional to the voltage applied to the MFC. Assuming deflection of the laminate is of the form:

$$w(x, y) = k \cdot x^2 \quad (2)$$

where  $w$  is the deflection of the laminate at a point relative to the flat laminate and  $x$  is the distance from the laminate edge in the  $x$ -direction. Knowing that maximum deflection ( $w_{\max}$ ) occurs at the mid-span ( $L/2$ ) it can be seen from Eq. (2) that the centre deflection of the laminate may be written as:

$$w_{\max}(L/2, 0) = k \cdot L^2/4 \quad (3)$$

From Eq. (3) it can be seen that maximum laminate deflection ( $w_{\max}$ ) is proportional to laminate curvature. As both central deflection ( $w_{\max}$ ) and voltage applied to the MFC (V) are proportional to laminate curvature ( $k$ ), it follows that central displacement ( $d$ ) must also be proportional to applied voltage. In this single state deformation mode the piezoelectric–laminate combination is in many ways similar to THUNDER and LIPCA actuators [30], which are also curved due to differing coefficients of thermal expansion

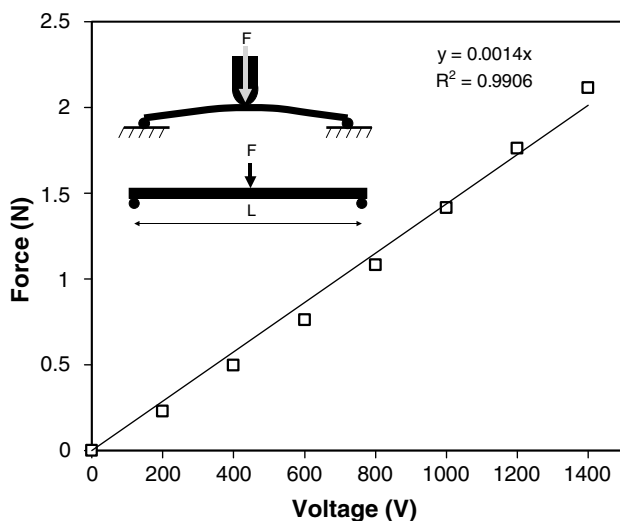


Fig. 3. Blocking force versus applied voltage. Cross-head displacement is fixed.

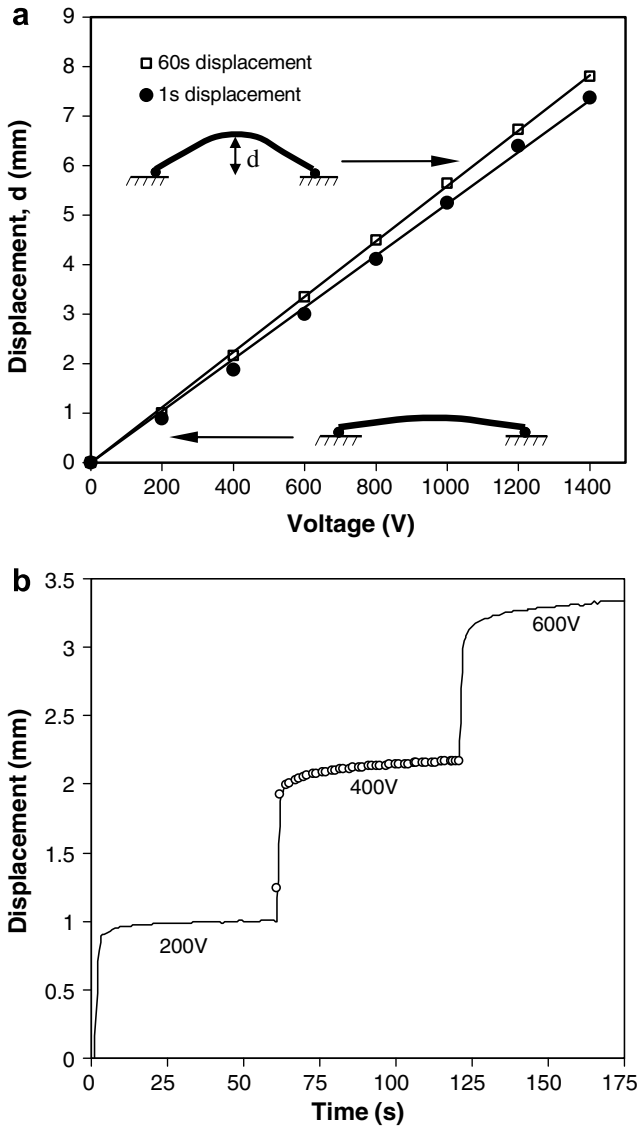


Fig. 4. (a) Centre free displacement versus applied voltage, displacement ( $d$ ) is central displacement at voltage  $V$  relative to its original position at 0 V; (b) creep displacement after application of voltage (solid line is experimental data, open circles represent fit based on Eq. (4)).

of individual layers in the actuators. These actuators also demonstrate linear relationship between deflection and applied voltage or electric field [30]. The thermally actuated active laminate of Asanuma [27] also exhibited linear relationship between laminate temperature, the analogous excitation for the laminate, and free deflection.

There is some creep (drift) of the displacement where the rate of drift decays with time. The degree of drift appears to increase as the applied voltage increases (Fig. 4a). Hysteresis and creep in piezoelectric materials, such as lead zirconate titanate (PZT), is thought to be due to a delayed response to domain switching. The creep response has a logarithmic shape over time [30,31] and is commonly observed when piezoelectric materials are subjected to conventional open-loop actuation with a rapid change in applied voltage.

The creep response has a logarithmic shape over time ( $t$ ) and follows Eq. (4) [32].

$$x(t) = x_0 \left[ 1 + \gamma \log \left( \frac{t}{0.1} \right) \right] \quad (4)$$

where  $x(t)$  is the piezoelectric actuator’s displacement (centre deflection) for any fixed input voltage,  $x_0$  is a nominal constant displacement value (namely the displacement 0.1 s after applying the input voltage) and  $\gamma$  is a creep factor which determines the logarithmic creep rate (percent change per time decade). The rate of the creep, and  $\gamma$ , are a function of the input voltage. Fig. 4b shows time deflection data for 200, 400 and 600 V, showing the creep in displacement. As an example, Eq. (4) is shown fitted to the data for 400 V with a good fit for a creep factor of 0.075; determined by graphical fitting of the data to a plot of  $x(t)$  versus  $\log_{10}(t/0.1)$ . Typical  $\gamma$  values for the data for 200–1400 V range from 0.03 to 0.08.

### 3.3. Blocking force-free deflection

While the maximum free deflection of the actuator is known (with no applied force) and the maximum blocking force is known (with no deflection), the response of the laminate under combined force generation and deflection are estimated using a ‘force-generation versus displacement’ diagram. If  $x_{\text{free}}$  is the free deflection,  $F$  is force and  $\Delta$  is actual displacement under combined electrical and mechanical loading, the relationship between them is given by Eq. (5) [28].

$$\Delta = x_{\text{free}} - \frac{F}{k_{\text{actuator}}} \quad (5)$$

where  $k_{\text{actuator}}$  is the stiffness of the actuator (N/mm). From Eq. (5), when  $\Delta = 0$  the blocking force  $F$  is  $k_{\text{actuator}} \cdot x_{\text{free}}$  and when  $F = 0$  the displacement  $\Delta$  is  $x_{\text{free}}$ .

Fig. 5 is a force-generation versus displacement diagram constructed using the free deflection and blocking force data discussed in Sections 3.1 and 3.2. The intercept points on the force ( $x$ )-axis as a function of voltage correspond to the blocking force data in Fig. 3, while the intercept points on the deflection ( $y$ )-axis correspond to the free deflection data (Fig. 4). For conditions of simultaneous displacement and force-generation (such as an actuator pushing against a spring of stiffness  $k_s$ ) a line is drawn between these two extreme points at each voltage (which is a line based on Eq. (5)). Since the gradient of the lines in Fig. 5 are  $-1/k_{\text{actuator}}$  the near approximate gradient suggests that laminate elastic modulus does not change significantly with applied voltage whilst in state A.

### 3.4. Force–displacement until snap-through

Fig. 6 shows the force–displacement behaviour of the piezoelectric–laminate combination as the cross-head in Fig. 2 is lowered at a constant rate, causing the laminate to snap-through from state A to state B under displacement

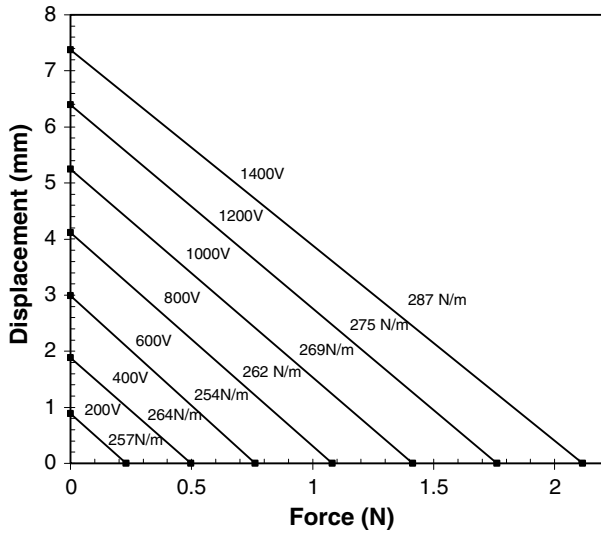


Fig. 5. Force-generation versus displacement as a function of applied voltage. Actuator stiffness based on gradient also indicated in N/m.

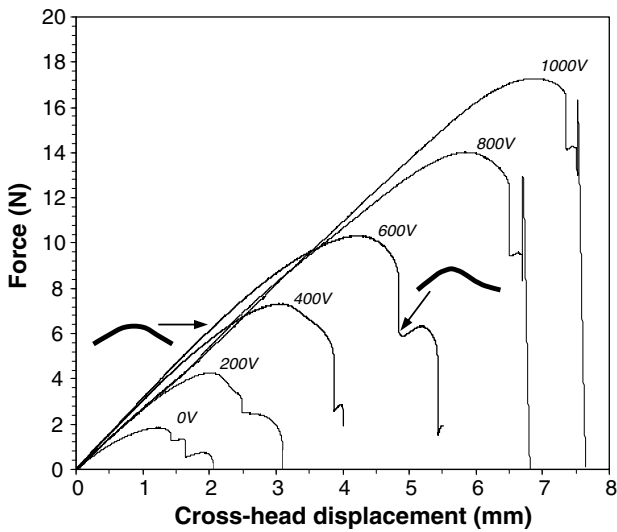


Fig. 6. Force versus cross-head displacement until snap-through from state A to state B for different voltages.

control. Cross-head displacement has been used in Fig. 6 since the total displacements exceed the measurement range of the laser (>5 mm). The force–displacement curves are initially linear but the gradient of the force–displacement curve decreases as the laminate begins to snap from state A to state B. From Fig. 6, the transition from state A to state B does not take place in a single stage. Potter et al. [33] have examined the process in detail and observed that snap-through does not occur immediately after a peak load, but rather a slow reduction in the load as one side of the sample reverses its curvature (see inset of Fig. 6). Snap-through (and a final rapid reduction in load) occurs when the other side of the laminate also reverses its curvature [33].

The stiffness of the piezoelectric–laminate combination can be calculated from the linear force–displacement characteristics during the initial 1 mm deflection of the laminate. Since the initial displacement was measured via the laser, the additional deflections of the test fixture are removed. The variation in stiffness of the piezoelectric–laminate combination with applied voltage is shown in Fig. 7. Compared to Fig. 5 (which shows no change in stiffness with voltage) the variation in stiffness with applied voltage is less clear. There is, however, a more significant change in the peak snap-through forces from state A to state B, which increases linearly with applied voltage (see Figs. 6 and 8). This can be explained by considering that voltage applied to the actuator results in an increase in the curva-

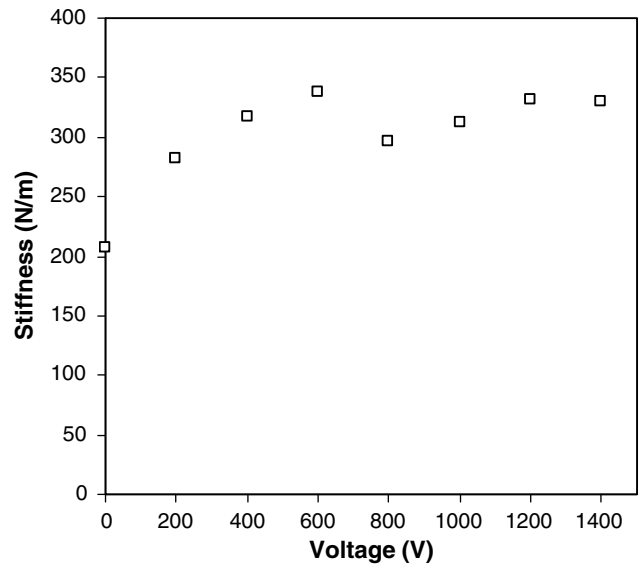


Fig. 7. Stiffness as a function of voltage from gradient of force-laser deflection curve.

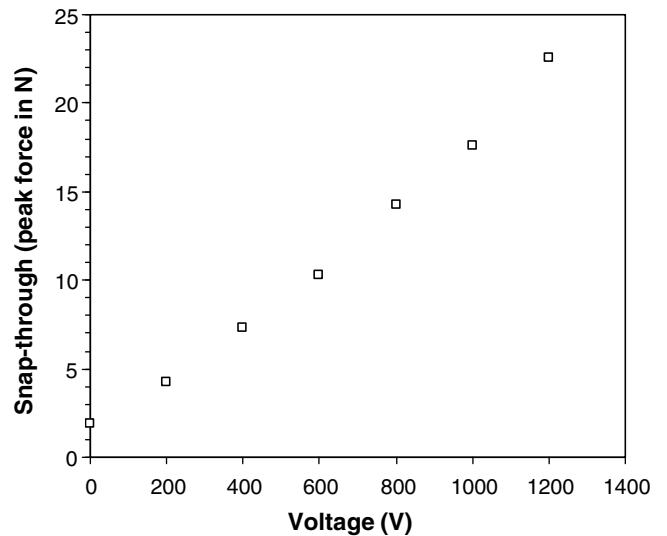


Fig. 8. Peak force for snap-through from state A to state B as a function of applied voltage.

ture and centre deflection of the laminate. Since the laminate stiffness is approximately constant but centre deflection is higher, a greater force is required to flatten the piezoelectric–laminate sufficiently to initiate snap-through from state A to state B.

#### 4. Conclusions

This paper has characterised the actuator properties of a bi-stable carbon fibre composite with a piezoelectric actuator bonded to its upper surface. An unsupported piezoelectric–laminate combination was evaluated in terms of its blocking force, free displacement and load–displacement characteristics. Linear relationships between blocking force and free displacement with applied voltage were observed when the laminate was actuated in a single deformation state. The creep of the structure was attributed to the characteristics of the piezoelectric material under open-loop control. Although no significant change in stiffness of the piezoelectric–laminate combination with applied voltage was observed, the force–displacement actuator characteristics indicate significant control of the snap-through force could be achieved by the application of voltage to the piezoelectric actuator.

#### Acknowledgements

The authors would like to thank UK Engineering and Physical Science Research Council (EPSRC) for funding part of this work.

#### References

- [1] Ramrakhyani DS, Lesieutre GA, Frecker M, Bharti S. Aircraft structural morphing using tendon-actuated compliant cellular trusses. *J Aircraft* 2005;42:1615–21.
- [2] Kudva JN. Overview of the DARPA Smart Wing Project. *J Intel Mat Sys Str* 2004;15:261–7.
- [3] Schultz MR, Hyer MW. Snap-through of unsymmetric cross-ply laminates using piezoelectric actuators. *J Intel Mat Sys Str* 2003;14:795–814.
- [4] Schultz M, Hyer MW, Brett Williams R, Keats Wilkie W, Inman DJ. Snap-through of unsymmetric laminates using piezocomposite actuators. *Comp Sci Technol* 2006;66:2442–8.
- [5] Gude M, Hufenbach W. Design of novel morphing structures based on bistable composites with piezoceramic actuators. *Mech Compos Mater* 2006;42:339–46.
- [6] Hufenbach W, Gude M, Czulak A. Actor-initiated snap-through of unsymmetric composites with multiple deformation states. *J Mater Process Tech* 2006;175:225–30.
- [7] Hufenbach W, Gude M, Kroll L. Design of multistable composites for application in adaptive structures. *Comp Sci Technol* 2002;62:2201–7.
- [8] Schultz MR. A new concept for active bistable twisting structures. In: *Proceedings of SPIE – the international society for optical engineering* 2005, vol. 5764. p. 241–52.
- [9] Bowen CR, Butler R, Jervis R, Kim HA, Salo AIT. Morphing and shape control using unsymmetrical composites. *J Intel Mat Sys Str* 2007;18:89–98.
- [10] Potter KD, Weaver PM. A concept for the generation of out-of-plane distortion from tailored FRP laminates. *Comp Part A – Appl S* 2004;35(12):1353–61.
- [11] Ren L, Parvizi-Majidi A. Model for shape control of cross-ply laminated shells using a piezoelectric actuator. *J Comp Mater* 2006;40:1271–85.
- [12] Hyer MW. Some observations on the cured shapes of thin unsymmetric laminates. *J Comp Mater* 1981;15:175–94.
- [13] Pirgon O, Wostenholm GH, Yates B. Thermal expansion at elevated temperatures IV. Carbon-fibre composites. *J Phys D* 1973;6:309–21.
- [14] Hahn HT. Residual stresses in polymer matrix composite laminates. *J Comp Mater* 1976;10:266–78.
- [15] Weitsman Y. Residual thermal stresses due to cool-down of epoxy resin composites. *J Appl Mech* 1997;46:563–7.
- [16] Hyer MW. Calculations of room temperature shapes of unsymmetric laminates. *J Comp Mater* 1981;15:296–310.
- [17] Bert CW, Mayberry BL. Free vibrations of unsymmetrically laminated anisotropic plates with clamped edges. *J Comp Mater* 1969;3:282–93.
- [18] Smart Materials Corporation, 2004, Macro Fiber Composites (Smart Doc # MFC-2.0-0504). [online] Available from: <http://www.smart-material.com/media/Publications/MFCdata%2013-3-web.pdf>.
- [19] Dang J, Tang Y. Calculation of the room-temperature shapes of unsymmetric laminates. In: *Proceedings of the international symposium on composite materials and structures*; 1986. p. 201–6.
- [20] Jun WJ, Hong CS. Cured shape of unsymmetric laminates with arbitrary lay-up angles. *J Reinf Plast Comp II* 1992;11(12):1352–66.
- [21] Hamamoto A, Hyer MW. Non-linear temperature–curvature relationships for unsymmetric graphite epoxy laminates. *Int J Solid Str* 1987;23:919–35.
- [22] Schlecht M, Schulte K, Hyer MW. Advanced calculations of the room-temperature shapes of thin unsymmetric composite laminates. *Comp Str* 1995;32:627–33.
- [23] Peeters LJB, Powell PC, Warnet L. Thermally-induced shapes of unsymmetric laminates. *J Comp Mater* 1996;30(5):603–26.
- [24] Schlecht M, Schulte K. Advanced calculations of the room-temperature shapes of unsymmetric laminates. *J Comp Mater* 1999;33(16):1472–90.
- [25] Ren L. Theoretical study on shape control of thin cross-ply laminates using piezoelectric actuators. *Comp Str* 2006;80/3:451–60.
- [26] Dano ML, Hyer MW. SMA-induced snap-through of unsymmetric fiber-reinforced composite laminates. *Int J Sol Str* 2003;40:5949–72.
- [27] Asanuma H, Haga O, Ohira J, Hakoda G, Kimura K. Proposal of an active composite with embedded sensor. *Sci Tech Adv Mat* 2002;3:209–16.
- [28] Cain M, Stewart M. The measurement of blocking force. National Physical Laboratory Report MATC(A)48 2001; Teddington, UK; ISSN: 1473 2734.
- [29] Gere JM, Timoshenko SP. *Mechanics of Materials*. 4th ed. PWS Publishing Company; 1997.
- [30] Yoon KJ, Shin S, Park HC, Goo NS. Design and manufacture of a lightweight piezo-composite curved actuator. *Smart Mater Struct* 2002;11:163–8.
- [31] Huang H, Tianshu Z, Oh JT, Hing P. Stress- and strain-relaxation in lead zirconate titanate based ceramics. *Mat Chem Phys* 2002;75:186–9.
- [32] Jung H, Shim JY, Gweon D. Tracking control of piezoelectric actuators. *Nanotechnology* 2001;12:14–20.
- [33] Potter K, Weaver P, Seman A, Shah S. Phenomena in the bifurcation of unsymmetric composite plates. *Composites Part A* 2007;38:100–6.